The resolution sensitivity of Northern Hemisphere blocking in four 25-km atmospheric global circulation models

R. Schiemann[1], P. Athanasiadis[6], M.-E. Demory[1], L. C. Shaffrey[1], J. Strachan[1], P. L. Vidale[1], M. S. Mizielinski[2], M. J. Roberts[2], M. Matsueda[3], M. F. Wehner[4], T. Jung[5]

[1]National Centre for Atmospheric Science, University of Reading, UK. [2]Met Office Hadley Centre, UK. [3]Atmospheric Physics, University of Oxford, UK. [4]Lawrence Berkeley National Laboratory, Berkeley, California, USA. [5]ECMWF, Reading, UK, and AWI, Bremerhaven, Germany. [6]CMCC, Bologna, Italy

National Centre for Atmospheric Science — NATURAL ENVIRONMENT RESEARCH COUNCIL

Met Office — NATURAL ENVIRONMENT RESEARCH COUNCIL

Joint Weather & Climate Research Programme

1. Introduction

The representation of atmospheric blocking has been shown to improve with climate model resolution both in controlled experiments (e.g., Matsueda et al., 2009) and across the CMIP5 ensemble (e.g., Anstey et al. 2013, Masato et al., 2013).

Here (Schiemann et al., 2017), we use ensembles of AMIP-style simulations with four GCMs at resolutions much higher (~25km grid spacing) than those typical in CMIP5. We evaluate the bias and resolution sensitivity of

- the location and frequency of blocking
- the association between blocking and mean-state biases (following Scaife et al. 2010)

2. Multi-model ensemble and experiments

IFS
- 91 levels
- AMIP-II SSTs
- ATHENA (Jung et al., 2012)

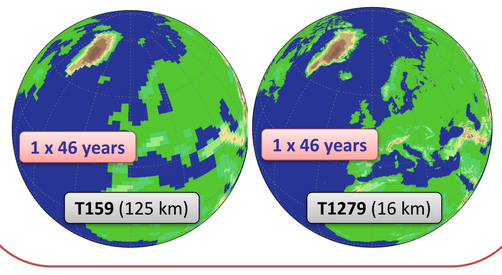

MRI-AGCM 3.2
- 63 levels
- AMIP-II SSTs

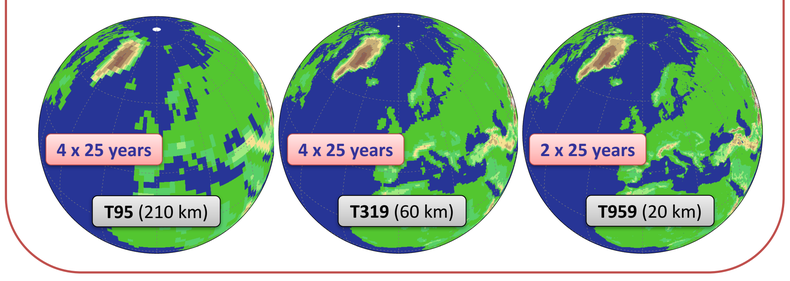

HadGEM3-GA3.0
- 85 levels
- OSTIA SSTs
- UPSCALE (Mizielinski et al. 2014)

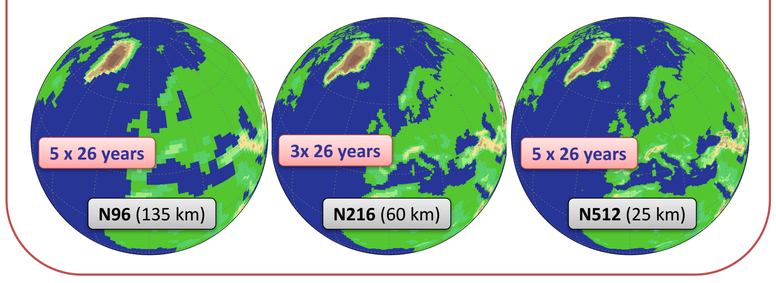

CAM5
- 30 levels
- AMIP SSTs
- Wehner et al. 2014

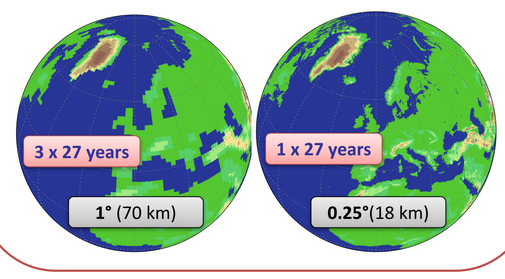

3. Blocking index

We use the two-dimensional 'AGP' index introduced by Scherrer et al. 2006. It is an extension to two dimensions of the index defined by Tibaldi and Molteni 1990. The identification of a blocking event at the reference latitude ϕ_0 is based on the daily 500hPa geopotential height field according to three criteria:

1) reversal of the climatological equator-pole geopotential height gradient to the south of the reference latitude $\frac{Z(\phi_o)-Z(\phi_s)}{\phi_o-\phi_s}>0$

2) westerlies, i.e. decreasing geopotential height with latitude, to the north of the reference latitude $\frac{Z(\phi_n)-Z(\phi_o)}{\phi_n-\phi_o}<-10\ \frac{\mathrm{m}}{^\circ\mathrm{lat}}$

3) persistence of 5 days or longer

Composite analysis shows the surface anticyclone and wave breaking typically associated with the block (Fig. 1).

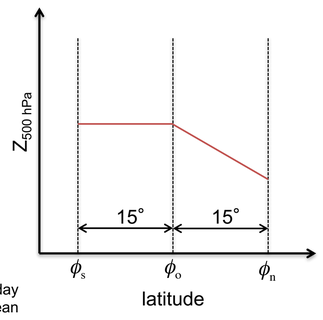

Fig. 1 (below): DJF (December – February) blocked-day composites. Left: Geopotential height at 500hPa (m). Right: Mean sea level pressure (hPa). Data: ERA-Interim (1979 – 2011).

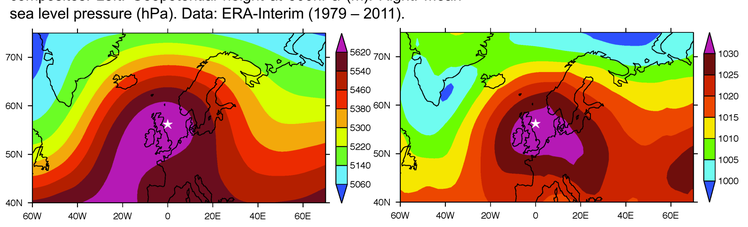

4. Blocking frequency and location

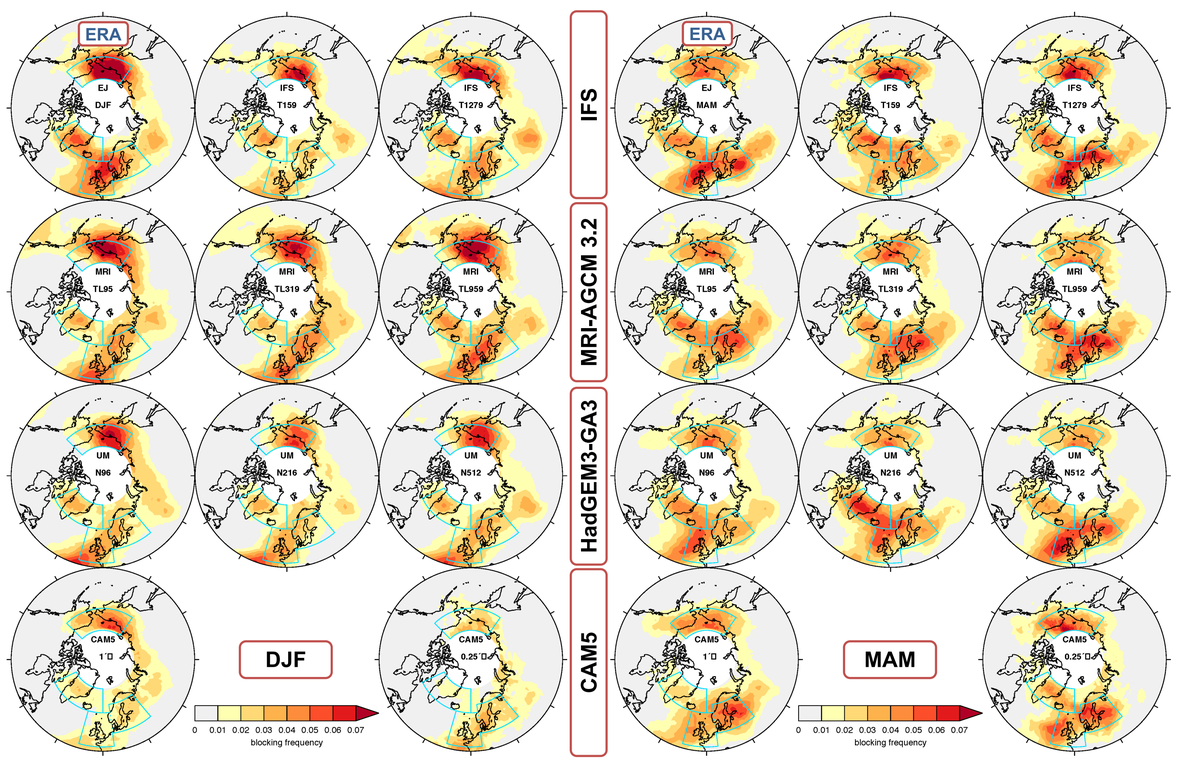

- robust (and significant, not shown) improvement in Atlantic blocking in MAM
- smaller improvement in DJF

Fig. 2: Frequency of blocked days in winter (left) and spring (right) for the four models (top to bottom). The verifying reanalysis (concatenation of ERA-40 and ERA-Interim) is shown in the top left panel.

5. Systematic assessment

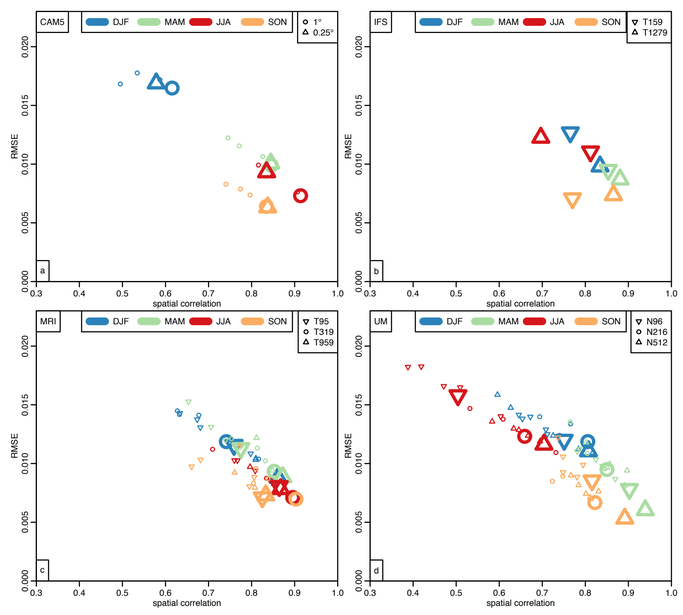

Fig. 3: Blocking frequency root-mean-square error and spatial correlation with respect to the reanalysis blocking frequency field shown in Fig. 2 for the Atlantic/European sector (80W–80E, 45–75N). Panels (a–d) are for the four different models, smaller symbols correspond to ensemble members and larger symbols to the ensemble mean.

- clear improvement with resolution overall, but variation between models/seasons
- internal variability is large, ensembles required

6. Mean and blocking biases

- bias-correct the Z500 field…

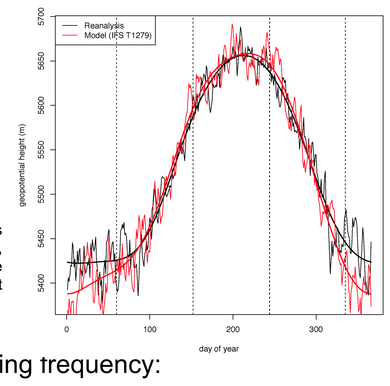

Fig. 4: Example of bias correction at one grid point (0E, 56N). The daily climatologies are low-pass filtered with a cutoff at 90 days.

- … and re-calculate the blocking frequency:

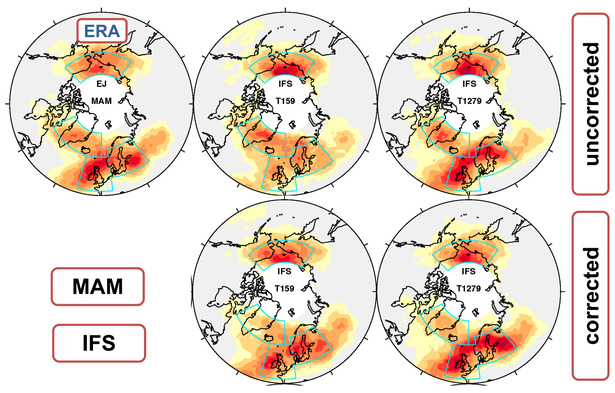

Fig. 5: top: Reanalysis and IFS blocking frequency as in Fig. 2. bottom: Blocking frequency obtained from bias-corrected geopotential height field. Colour bar as in Fig. 2.

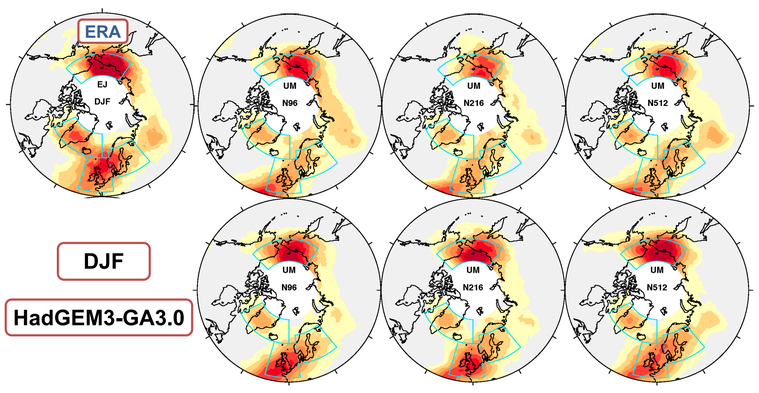

Fig. 6: As Fig. 4, but for DJF and the HadGEM3-GA3.0 model.

- MAM blocking bias largely associated with mean-state bias for the IFS model (and also HadGEM3-GA3.0, not shown)
- DJF blocking bias partly associated with mean-state bias in HadGEM3-GA3

7. Outlook

PRIMAVERA

An ensemble of AMIP-style simulations has been evaluated in this study. Our results will be extended to the multi-model ensemble of coupled high-resolution simulations currently produced in the PRIMAVERA project. PRIMAVERA is the European contribution to CMIP6-HighResMIP (Haarsma et al. 2016).

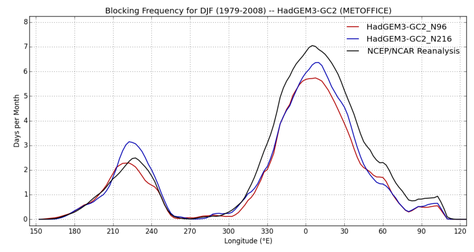

Fig. 7: Frequency of occurrence of instantaneous blocking in wintertime (DJF) along the observed Central Blocking Latitude, as in Athanasiadis et al. (2014), for HadGEM3-GC2. Mean bias correction has been applied prior to the identification of blocking events as in Scaife et al. (2010).

- preliminary analysis suggests improvement at N216 resolution in HadGEM3-GC3

8. Summary

Atlantic blocking simulated in global atmospheric models remains sensitive to resolution as the grid spacing is reduced to about 25km, yet the sensitivity depends on the season: While there is a robust and significant improvement in simulated Atlantic blocking in spring, winter and summer blocking continues to be underestimated at high-resolution and not all models show improvement. In autumn, the blocking frequency is fairly well captured at all resolutions. The improvement with resolution in spring is associated with a better model mean state. The winter bias can only be partly explained with the mean-state bias. Pacific blocking does not systematically depend on model resolution.

References

Athanasiadis et al. (2014): J. Climate, doi: 10.1175/JCLI-D-14-00291.1
Anstey, J A, et al. (2013): J. Geophys. Res., 118, 3956 – 3971, doi: 10.1002/jgrd.50231
Jung, T, et al. (2012): J. Climate, 25, 3155 – 3172, doi: 10.1175/JCLI-D-11-00265.1
Haarsma, R J, et al. (2016): Geosci. Model Dev., doi:10.5194/gmd-9-4185-2016
Masato, G, et al. (2013): J. Climate, 26, 7044 – 7059, doi: 10.1175/JCLI-D-12-00466.1
Matsueda, M, et al. (2009): J. Geophys. Res., 114, D12114, doi: 10.1029/2009JD011919
Mizielinski, M S, et al. (2014): Geosci. Model Dev., doi:10.5194/gmd-7-1629-2014
Scaife, A A, et al. (2010): J. Climate, 23, 6143 – 6152, doi: 10.1175/2010JCLI3728
Scherrer, S C, et al. (2006): Int. J. Climatol., 26, 233 – 249, doi: 10.1002/joc.1250
Schiemann, R, et al. (2017): J. Climate, doi: 10.1175/JCLI-D-14-00291.1 (this study)
Tibaldi, S, and Molteni, F, (1990): Tellus A, 42, 343 – 365, doi: 10.1034/j.1600-0870.1990.t01-2-00003.x
Wehner, M F, et al. (2014): J. Adv. Earth Syst. Sci., doi: 10.1002/2013MS000276